

Stability and Electrocatalytic Activity for Oxygen Reduction in WC+Ta catalyst

Kunchan Lee^a, Akimitsu Ishihara^b, Shigenori Mitsushima^a, Nobuyuki Kamiya^{a,1},
Ken-ichiro Ota^{a,*},¹

^a*Yokohama National University*, ^b *CREST-JST*

*Department of Energy and Safety Engineering, Yokohama National University
79-5 Tokiwadai, Hodogaya-ku, Yokohama 240-8501, Japan*

Abstract

We have prepared a Ta-added tungsten carbide (WC+Ta) in order to obtain superior characteristics for pure tungsten carbide in stability and electrocatalytic activity for oxygen reduction under high acid and potential environments. The stability and the electrocatalytic activity were electrochemically investigated and compared to the pure WC. The surface conditions of the catalysts were analyzed by X-ray photoelectron spectroscopy (XPS). From the electrochemical measurements, it was found that the stability of the tungsten carbide was significantly increased by the addition of tantalum compared to the pure WC. The electrocatalytic activity in the WC+Ta catalyst was observed at a potential of 0.8V (vs. DHE) or less noble potential. This value was 0.35V higher than that of the pure WC. The enhanced stability and the electrocatalytic activity at high potential were evidenced by an XPS analysis. The enhanced stability was due to the formation of the W-Ta alloy in the WC+Ta catalyst. Since this alloy formed a stable passive oxide film on the catalyst surface, the oxidation of the carbide was restrained. The carbidic tungsten that was not oxidized on the surface and/or sub-surface is considered to make this catalyst have an electrocatalytic activity at a higher positive potential.

Keywords: Non-noble electrocatalyst; Ta-added tungsten carbide; Oxygen reduction; Corrosion resistance; Electrocatalyst design

1. Introduction

Recently, the development of new non-noble catalysts has been strongly demanded in electrochemical fields such as electrolysis and fuel cells. In particular, since the polymer electrolyte fuel cell (PEFC) has recently attracted increasing interest as a new power system, the necessity with respect to the development of a non-noble electrocatalyst also increases more and more for its commercialization and mass production.

Transition metal carbides have been widely studied as non-noble catalysts because of their electrochemical properties and electrical conductivities [1-13]. In particular, the reports [4,5,7,8] that tungsten carbide exhibits a platinum-like behavior with respect to the chemisorption of hydrogen and oxygen have increased its applicability as an alternative electrocatalyst of Pt. Recently, there have been several trials with respect to the transition metal carbides, such as the tungsten carbide, as the non-noble electrocatalysts in the PEFC [2,9,14-16].

The research results [9,16-20] showed that the tungsten carbides exhibited a high catalytic activity for the oxidation of hydrogen or methanol in acid solutions and may provide us with new possibilities with respect to the tungsten carbide as the anode electrocatalyst of PEFC. In the work of Trassatti et al. [1], it was also found that the tungsten carbide was superior to the other transition metal carbides for the electrocatalytic activity of oxygen reduction in acid solution. This fact indicates that this catalyst can also become a possible candidate as the oxygen reduction electrocatalyst in a PEFC. However, it is very difficult to use a pure tungsten carbide as the oxygen reduction electrocatalyst, because this material exhibits a very low corrosion resistance in high acid and positive electrode potential conditions [3,21-24]. In order to use the carbides as the oxygen reduction catalyst, these materials must be modified in order to have superior characteristics in both the stability and the electrocatalytic activity in a highly corrosive atmosphere. As a method to increase the stability of the carbide catalysts, the addition of a second metal to the carbides can be applied in the electrocatalyst design. It is expected that this method might allow the carbide catalyst to have both better stability and the electrocatalytic activity characteristics. In other words, the additive might contribute to the stability of the carbide catalyst and the electrocatalytic activity might be assigned to the carbidic metal.

Various methods of second metal addition can be used in the synthesis of carbide and different characteristics are also expected according to the different methods. We have prepared a second metal-added tungsten carbide using the R.F. sputtering method in order to apply carbide materials to the oxygen reduction catalyst. Tantalum metal was used as the second metal, since this metal is well known to increase the corrosion resistance in alloys. The Ta-added tungsten carbide (WC+Ta) is expected to have enhanced stability in a highly corrosive atmosphere. Moreover, the carbidic metal is expected to contribute to the electrocatalytic activity of this modified catalyst. In this study, the WC+Ta catalyst was compared to the pure tungsten carbide (WC) with respect to the stability and the electrocatalytic activity for oxygen reduction, and the applicability of our electrocatalyst design to carbide materials was discussed.

2. Experimental

2.1. Synthesis of tungsten carbides

The WC+Ta or the WC catalyst was deposited onto a glassy carbon rod substrate (ϕ 5mm) by R.F. sputtering sintered WC and tantalum targets in an Ar atmosphere. The WC and the tantalum targets were 99% and 99.9%, respectively. Prior to the sputter-deposition, the surface of the glassy carbon rod was polished to a mirror-finish using Fuji film lapping tape (LT-06000). The setup of the WC and the tantalum targets are schematically represented in Fig. 1. In order to add tantalum to the WC, after the tantalum targets (thickness = 0.1mm, area=1cm²) were put on the WC target, the tantalums were sputtered together with the tungsten carbide. The composition of the tantalum was controlled by changing the area of the tantalum target. The sputtering pressure in the chamber was less than 1x10⁻⁴ Pa. Prior to the sputter-deposition, the targets were cleaned by pre-sputtering for 10 minutes in order to remove any possible target

contaminations. The chemical composition of the sputter-deposited carbide was determined by energy dispersive X-ray analysis (EDX). The WC+Ta sample was controlled to have the atomic ratio of W:Ta=0.66:0.34. The surface observations before and after the electrochemical measurement were also determined by X-ray photoelectron spectroscopy (XPS) using Mg K_{α} radiation. The electron binding energy of the XPS was referenced to the Au $4f_{7/2}$ at 84eV and the C 1s of a carbon contaminant at 285eV [26]. The microstructure of the sputter-deposited carbide was confirmed by X-ray diffraction (XRD) using Cu K radiation.

2.2. Electrochemical measurements

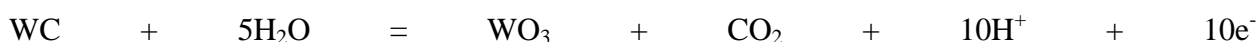
The stability in an acidic electrolyte and the electrocatalytic activity for the oxygen reduction were investigated by electrochemical measurements. The electrochemical measurements were carried out in a solid-state cell with Nafion[®] 117 as the electrolyte as shown in Fig. 2 [27] in order to apply the tungsten carbide to the electrocatalyst of the PEFC. The sputter-deposited WC+Ta or WC was fixed at the position of the working electrode. A dynamic hydrogen electrode (DHE) and a platinum foil with Pt black were used as the reference electrode and the counter electrode, respectively. The electrolyte membrane was sandwiched between the working electrode on the upper side and the counter electrode on the other side. The contact pressure of the working electrode on the polymer electrolyte was controlled by a strain control screw and measured with a strain gauge. The electrode contact pressure was controlled at 1 kg/cm². Oxygen or nitrogen gas fed into the cell was humidified by passing through a bubbler and the temperature of the bubbler was controlled at 20°C higher than the cell temperature in order to attain a saturated relative humidity.

3. Results and Discussion

3.1. Electrochemical measurements

Figure 3 shows the XRD patterns of the sputter-deposited WC+Ta catalyst. The sputter-deposited catalyst has a poor crystalline, that is, almost amorphous structure, since the sharp crystalline peaks are not observed in the XRD patterns. This appears to be consistent with the literature indicating that the sputter-deposited tungsten carbide becomes amorphous [19,28,29].

Figure 4 shows the steady-state cyclic voltammograms for the WC and the WC+Ta on the Nafion[®] under a N₂ atmosphere. A significant anodic current above 0.5V (vs. DHE) in the WC catalyst is observed according to the anodic polarization, while the WC+Ta catalyst shows no change in the anodic current as shown in Fig. 4(a). In addition, the WC catalyst also exhibits large changes in the anodic and cathodic currents at elevated temperature as shown in Fig. 4(b). The oxidation of the tungsten carbide by the anodic polarization is considered as follows [3,21,23].



(1)

According to the anodic polarization, the tungsten in the tungsten carbide oxidizes to tungsten oxide. Since tungsten is one of the so-called valve metals that form passive oxides upon anodic polarization in an acidic media, passive oxides such as WO_3 might be formed on the tungsten carbide surface. On the other hand, the carbon in the tungsten carbide is oxidized on the catalyst surface with the evolution of carbon dioxide over the potential of 0.8V [3,21,23]. The tantalum is also expected to form a passive oxide film on the surface, because this metal is also a valve metal [15,25]. Although passive oxides are formed on the surface of both catalysts, it was found that they exhibit different characteristics in the cyclic voltammograms.

In order to obtain the characteristics of the electrocatalytic activity for the oxygen reduction and the stability, slow scan voltammetry was carried out under N_2 and O_2 atmospheres. Figure 5 shows the slow scan voltammograms for the WC and the WC+Ta under each gas atmosphere. The WC catalyst exhibited anodic currents corresponding to the oxidation of the tungsten above 0.45V (vs. DHE) and the oxidation of the carbon at a potential of 0.8V (vs. DHE) under the N_2 atmosphere. On the other hand, the WC+Ta catalyst exhibited no large anodic current up to 1.0V under the N_2 atmosphere. In particular, the anodic current corresponding to the carbon oxidation was also not observed at 0.8V in the WC+Ta catalyst. These results indicate that the corrosion resistance of the tungsten carbide is increased by the addition of tantalum similar to what we expected in the electrocatalyst design. Therefore, the tantalum might play an important role in increasing the stability of the carbide.

Since the tungsten and the tantalum form a passive oxide on the surface of the catalyst as mentioned above, the behavior of the cathodic reduction of the passive oxides must be considered in order to electrochemically evaluate the electrocatalytic activity for the oxygen reduction. In the case of the WC catalyst, the increase in the cathodic current is observed at 0.4V to 0.2V according to the cathodic polarization under the N_2 atmosphere as shown in Fig. 5. This behavior might be due to the cathodic reduction of the tungsten oxide anodically formed on the surface of the catalyst [21]. On the other hand, the WC+Ta catalyst showed no increase in cathodic current according to the cathodic polarization. It is very difficult to evaluate the electrocatalytic activity of the WC catalyst for the oxygen reduction when comparing the N_2 and O_2 atmospheres, since the cathodic reduction of the oxide also occurs in the O_2 atmosphere. On the other hand, it is possible to estimate the electrocatalytic activity of the WC+Ta catalyst for the oxygen reduction from a comparison of the N_2 and O_2 atmosphere results, because the cathodic reduction current might be not included in the cathodic current. The apparent difference between the N_2 and O_2 atmospheres in the WC+Ta catalyst was observed in the cathodic currents. In the O_2 atmosphere, the onset potential of the oxygen reduction was observed at about 0.8V (vs. DHE). This potential was about 0.35V higher than that of the WC catalyst. This result reveals that the WC+Ta catalyst has an electrocatalytic activity for the oxygen reduction reaction, although it is not significant.

Figure 6 shows the potentiostatic curves for each sample at 0.6V under an O_2 atmosphere.

The potential step was carried out after holding the electrode potential at open circuit potential for 30 minutes. A stable cathodic current was observed in the WC+Ta catalyst, while the WC catalyst exhibited an anodic current at this potential. Since a 0.6V electrode potential is the oxidation potential of the tungsten carbide, if the oxygen reduction reaction and the oxidation reaction of the carbide on the surface of the WC+Ta catalyst simultaneously occur, it is considered that the stationary current might not be obtained throughout the entire potentiostatic time. Therefore, it can be seen that the oxygen reduction reaction on the surface of this catalyst stably occurs without the oxidation of the carbide.

The enhanced stability and the oxygen reduction activity at a high positive potential that were observed in the WC+Ta catalyst can be caused by several alloy reactions between the tungsten carbide and the second metal, i.e., tantalum. The alloy reactions between the tungsten carbide and the tantalum by a sputtering process can be expected as follows. The tantalum can combine with the carbon and/or the tungsten of the tungsten carbide. If the tantalum combines with the carbon of the tungsten carbide, the tantalum carbide (TaC_x) might be formed. The tungsten of the tungsten carbide can also combine with the tantalum during the sputtering process and they might form a W-Ta alloy. Therefore, these alloy reactions might allow the TaC_x and the W-Ta alloy to exist in the sputter-deposited WC+Ta catalyst.

Figure 7 shows the change in the open circuit potential up to 1000 minutes under the O_2 atmosphere in each alloy that is expected in the alloy reactions between the tungsten carbide and the tantalum additive. With the changes in the open circuit potentials, different characteristics were observed. The W-Ta alloy exhibited the highest open circuit potential and this value was higher than those of the tungsten and the tantalum metals. This characteristic is in good agreement with the report of Hashimoto [25]. It has been reported that the high stability of the W-Ta alloy is due to the formation of a stable passive oxide according to their synergetic effect [25]. TaC and/or Ta metal showed a higher corrosion resistance than WC and/or W metal. It was found that the carbidic metals exhibited a behavior different from the non-carbidic metals with respect to the changes in the open circuit potential. The open circuit potential values in the non-carbidic metals showed a significant rise in the first 200 minutes. On the other hand, the carbidic metals such as WC and TaC exhibited constant values from the initial time. The WC+Ta catalyst exhibits a characteristic similar to the non-carbidic metals concerning the change in the open circuit potential and the open circuit potential between the W-Ta alloy and Ta or W metal. These results lead us to consider that the WC+Ta catalyst might consist of the carbidic metal and the non-carbidic metals such as the W-Ta alloy, W and Ta as mentioned above. The X-ray photoelectron spectroscopy was carried out in order to elucidate the alloy composition of the WC+Ta catalyst.

3.2. X-ray photoelectron spectroscopy (XPS) analysis

Figure 8 shows the XPS peaks for W 4f, Ta 4f and C 1s in the as-deposited WC and WC+Ta catalysts. The two W 4f doublets in the W 4f peaks of the WC catalyst are observed as shown

in Fig. 8(a). The W $4f_{7/2}$ and the W $4f_{5/2}$ peaks corresponding to the binding energy of 31.6eV and 33.7eV, respectively, are assigned to the carbidic tungsten. These values are in good agreement with the literature values [8,30,31]. The W $4f_{7/2}$ and the W $4f_{5/2}$ peaks corresponding to 35.6eV and 37.1eV are related to WO_3 [32]. It is considered that the oxidic tungstens of the surface were formed by the oxidation of the carbidic tungsten, since the sample was transferred from the sputtering equipment into the XPS apparatus. On the other hand, the W $4f_{7/2}$ corresponding to carbidic tungsten in the WC+Ta catalyst was observed at the binding energy of 31.4eV that was 0.2eV lower than that of the WC catalyst. The oxidic tungsten was also observed on the surface of this catalyst. The XPS peaks of the C 1s observed on the as-deposited surface are composed of several types of carbons as shown in Fig. 8(b). The binding energy of 283.2eV might be associated with the carbidic carbon that chemically bonds to the tungsten [8,30,31] and was observed in both catalysts. The binding energy of 285eV corresponds to the carbon contaminations of the sample surface [26]. The C 1s peaks due to surface adsorbates such as CO, CO_2 and hydrocarbons were detected on the as-deposited surfaces.

The shift of the W 4f peaks corresponding to the carbidic tungsten to lower the binding energy in the WC+Ta catalyst might be attributed to alloying the WC and Ta metal as expected above. It is difficult to detail the condition of the as-deposited surface due to the contaminations and the oxides on the surface. In particular, the W 4f and Ta 4f peaks in the oxidic states of the WC+Ta catalyst are located close to each other and/or partially overlapped. Therefore, the surfaces of the catalysts were etched by Ar^+ ion sputtering in order to exactly analyze the alloy condition. Figure 9 shows the XPS spectra for the W4f and the Ta 4f on clean surfaces. After etching the surface, the peaks due to the oxides and contaminations were not observed. However, the W $4f_{7/2}$ peak in the WC+Ta catalyst is 0.2eV lower than that of the WC catalyst like the as-deposited surfaces as shown in Fig. 9(a). The W 4f peaks were deconvoluted using a Lorentzian-Gaussian function and separated into two types of tungstens with different electron states which corresponded to 31.6eV and 31.2eV, respectively. The W $4f_{7/2}$ peak of 31.6eV must correspond to the carbidic tungsten. On the other hand, since the W $4f_{7/2}$ peak of 31.2eV is not related with the metallic state ($W^0 4f_{7/2} = 31.4eV$) [12,32] as well as the carbidic state, this result means that there exists tungsten with different electron state from these electron states. In the case of the tantalum, the Ta 4f peaks are located at a position intermediate between the metallic and the carbidic states as shown in Fig. 9(b). These peaks were also deconvoluted into three different electron states; i.e., carbidic, metallic and intermediate states (between carbidic and metallic states). The presence of the tungsten and the tantalum with various electron states indicates that the WC+Ta catalyst might consist of various alloys. In accordance with the work of Hashimoto et al., the shifts in the binding energies for $W^0 4f$ and $Ta^0 4f$ were reported in the W-Ta alloys [25]. The peak shifts in the W-Ta alloy can be explained by the charge transfer from Ta to W, since the tungsten is more electronegative than the tantalum. The $W^0 4f$ peak decreases into a lower binding energy, while the $Ta^0 4f$ peak

increases into a higher binding energy. Accordingly, the W and the Ta with lower and higher electron states than the metallic state, respectively, must be related to the formation of the W-Ta alloy. The presence of the shifted W 4f and Ta 4f in the WC+Ta catalyst is attributed to the charge transfer of the Ta to the W due to the formation of the W-Ta alloy. When the tungsten combines with tantalum, the carbon will be separated from the tungsten carbide. A part of the carbons separated from the tungsten carbide are considered to recombine with the Ta, since the TaC_x is observed in the WC+Ta catalyst. The presence of the tantalum with the metallic state (Ta⁰ 4f) means that the metallic tantalum independently exists in the WC+Ta catalyst. These results are in good agreement with the alloy reaction expected in Fig. 7. Figure 10 shows the XPS spectra for the carbons in the WC+Ta catalyst after Ar⁺ etching. Two C 1s peaks with different electron states were observed on the clean surface. The C 1s peak of 283.2eV corresponds to the carbidic carbon. However, the binding energy of another C 1s peak is located at 284.6eV and this value is 0.4eV lower than that of the carbon contamination compared with the as-deposited surface. Therefore, this carbon is considered to not be the carbon contamination but a part of the carbons separated from the tungsten carbide. From these results, it is expected that the following alloy reactions will occur during simultaneously sputtering the tungsten carbide and the tantalum additive.

$$\text{WC} + \text{Ta} \rightarrow \text{WC} + \text{W-Ta alloy} + \text{TaC}_x + \text{Ta} + \text{C} \quad (2)$$

From these alloy reactions, the tungsten carbide might homogeneously exist together with the W-Ta alloy, TaC_x and Ta. The ratio of the tungsten alloyed with the tantalum is ca. 30% in total tungsten, and the tantalum of ca. 60% in total tantalum combines with the tungsten. In particular, since the W-Ta alloy has a higher corrosion-resistance due to its stable passive oxide, the presence of the W-Ta alloy in the WC+Ta catalyst definitely proves why this catalyst exhibits enhanced stability compared to the WC catalyst.

Figure 11 shows the XPS spectra for the W 4f and the Ta 4f after the electrochemical measurements. The XPS peaks for the carbidic tungsten in the WC catalyst were almost not observed after the electrochemical measurements. On the other hand, on the surface of the WC+Ta catalyst, the carbidic tungsten as well as the oxidic tungsten was observed after the electrochemical measurements. Most of the tantalum was also oxidized into the oxidic state, although a small portion of carbidic tantalum was observed. The oxidic tungsten and tantalum decrease the electron conductivity of the electrocatalyst surface because of their passivation. In addition, these passive oxides might make the oxygen reduction reaction to hardly occur on the surface and /or sub-surface. Consequently, the electrocatalytic activity observed in the WC+Ta catalyst is considered to be due to the carbidic tungsten that exists on the surface, since the tantalum carbide and the W-Ta alloy that are observed on the surface of the WC+Ta catalyst exhibit a very lower electrocatalytic activity for the oxygen reduction reaction compared to the WC+Ta catalyst as shown in Fig. 12.

Finally, from our results, it is expected that the other second metal-added carbides can also have better characteristics in both the stability and the electrocatalytic activity than their pure

carbides under high acid and potential environments such as what we have expected in the electrocatalyst design. In this study, however, it was found that the stability and the electrocatalytic activity of the carbide were sensitively affected by the second metal content. Therefore, further investigations into the preparation of the carbide catalysts are necessary in order to confirm the applicability of the carbide material to the electrocatalyst.

4. Conclusions

In our study, we prepared a modified tungsten carbide (WC+Ta) using R.F sputtering method in order to obtain superior characteristics compared to the pure tungsten carbide in terms of stability and electrocatalytic activity. The stability and the electrocatalytic activity were electrochemically investigated and compared to the pure WC. The surface conditions of the catalysts were analyzed by X-ray photoelectron spectroscopy (XPS). From the electrochemical measurements, it was found that the corrosion resistance of the tungsten carbide was significantly increased by the addition of tantalum when compared to the pure WC. The electrocatalytic activity for the oxygen reduction in the WC+Ta catalyst was also observed up to a high positive potential (0.8V vs. DHE) at which the pure WC was oxidized. The enhanced stability and the catalytic activity at high potential were evidenced by the XPS analysis. It was found that the enhanced stability was due to the formation of the W-Ta alloy in the WC+Ta catalyst. Since the W-Ta alloy formed a stable passive oxide film on the surface of the WC+Ta catalyst, the oxidation of the carbidic tungsten was considered to be restrained. In addition, the carbidic tungsten that existed on the surface and/or sub-surface led this catalyst having an electrocatalytic activity at a higher positive potential.

In this paper, it is considered that the new applicability of an electrocatalytic design with respect to the carbide materials was proved through the preparation of the Ta-added tungsten carbide, although we do not exactly know the mechanism of the oxygen reduction reaction in this catalyst. This electrocatalyst design concept will be expected to increase the applicability of the transition carbides to the electrocatalyst materials in the electrochemical fields such as fuel cells and electrolysis.

References

- [1] F. Mazza, S. Trassatti, J. Electrochem. Soc. 110 (1963) 847.
- [2] H. Binder, A. Kohling, W. Kuhn, W. Lindner, G. Sandstende, Nature 224 (1969) 1299.
- [3] H. Yoneyama, M. Kaneda, H. Tamura, Denkkagaku 41 (1973) 719.
- [4] R. B. Levy, M. boudart, Science 181 (1973) 547.
- [5] L. H. Bennett, J. R. Cuthill, A. J. McAlister, N. E. Erickson, Science 184 (1974) 563.
- [6] P. N. Ross, Jr., P. Stonehart, J. Catalysis 39 (1975) 298.
- [7] J. E. Hoston, G. E. Laramore, R. L. Park, Science 185 (1974) 258.
- [8] R. J. Colton, J. J. Huang, J. W. Rabalais, Chemical Physics Letters 34 (1975) 337.
- [9] P. N. Ross, Jr., P. Stonehart, J. Catalysis 48, (1977) 42.

- [10] I. Kojima, E. Miyazaki, Y. Inoue, I. Yasumori, *J. Catalysis* 59 (1979) 472.
- [11] J. Lemaitre, B. Vidick, B. Delmon, *J. Catalysis* 99 (1986) 415.
- [12] L. Leclercq, M. Provost, H. Pastor, J. Grimblot, A. M. Hardy, L. Gengembre, G. Leclercq, *J. Catalysis* 117 (1989) 371.
- [13] S. T. Oyama, *Catalysis today* 15 (1992) 179.
- [14] R. Cote, G. Lalonde, G. Faubert, D. Guay, J. P. Dodelet, G. Denes, *J. New Mat. Electrochem. Systems* 1 (1998) 7.
- [15] G. T. Burstein, D. R. McIntyre, A. Vossen, *Electrochemical and Solid-State Lett.* 5 (2002) A80.
- [16] D. R. McIntyre, G. T. Burstein, A. Vossen, *J. Power Sources* 107 (2002) 67.
- [17] D. V. Sokolsky, V. Sh. Palanker, E. N. Baybatyrov, *Electrochimica Acta* 20 (1975) 71.
- [18] H. Okamoto, G. Kawamura, A. Ishikawa, T. Kudo, *J. Electrochem. Soc.* 134 (1987) 1649.
- [19] K. I. Machida, Michio Enyo, *J. Electrochem. Soc.* 137 (1990) 871.
- [20] G. Bronoel, E. Museux, G. Leclercq, L. Lelercq, N. Tassin, *Electrochimica acta* 36 (1991) 1543.
- [21] J. D. Voorhies, *J. Electrochem. Soc.* 119 (1972) 219.
- [22] H. Binder, A. Kohling, W. Kuhn, W. Lindner, G. Sandstende, *Nature* 224 (1969) 1299.
- [23] P. Zoltowski, *Electrochimica acta* 31 (1986) 103.
- [24] H. Scholl, B. Hofman, A. Rauscher, *Electrochimica Acta* 37 (1992) 447.
- [25] J. Bhattarai, E. Akiyama, H. Habazaki, A. Kawashima, K. Asami, K. Hashimoto, *Corrosion Science* 40 (1998) 757.
- [26] D. Briggs, M. P. Seah, *Practical Surface Analysis 2nd ed., Auger and X-ray Photoelectron Spectroscopy*, WILEY, (1990).
- [27] A. Parthasarathy, C. R. Martin, S. Srinivasan, *J. Electrochem. Soc.* 138 (1991) 916.
- [28] B. Trindade, M. T. Vieira, E. Bauer-Grosse, *Acta mater.* 46 (1998) 1731.
- [29] B. Trindade, M. T. Vieira, *Thin solid films* 322 (1998) 68.
- [30] S. J. Wang, H. Y. Tsai, S. C. Sun, *Thin Solid Films* 394 (2001) 180.
- [31] S. H. Koutzaki, J. E. Kraznowski, J. J. Nainaparampil, *Metall. & Mater. Transaction A* 33 (2002) 1579.
- [32] S. S. Perry, H. C. Galloway, P. Cao, E. J. R. Mitchell, D. C. Koeck, C. L. Smith, M. S. Lm, *Applied Surface Science* 180 (2001) 6.

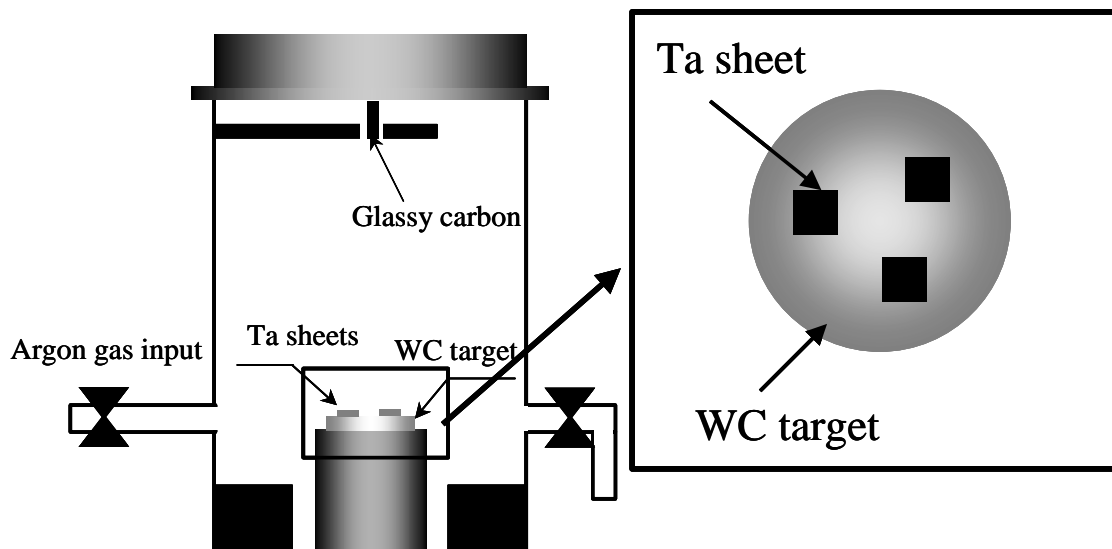


Fig. 1. Schematic drawing of R.F sputtering system.

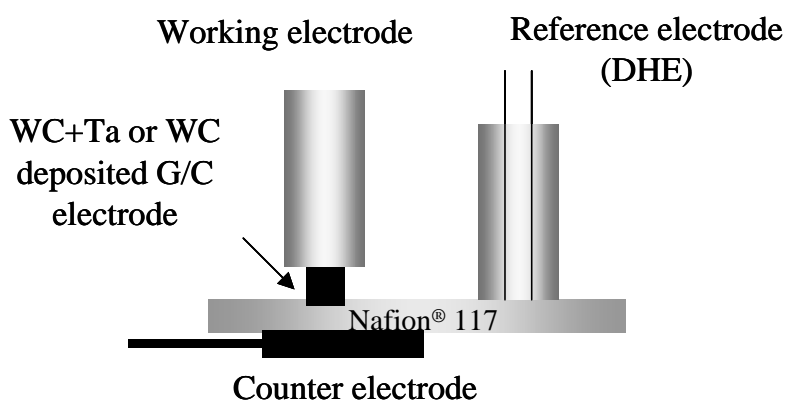


Fig. 2. Schematic drawing of solid-state cell.

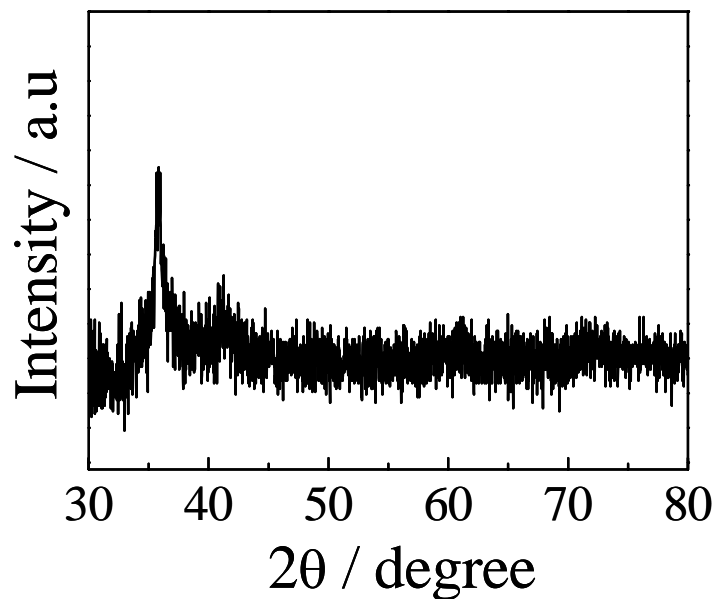


Fig. 3. X-ray diffractogram of as-deposited WC+Ta catalyst.

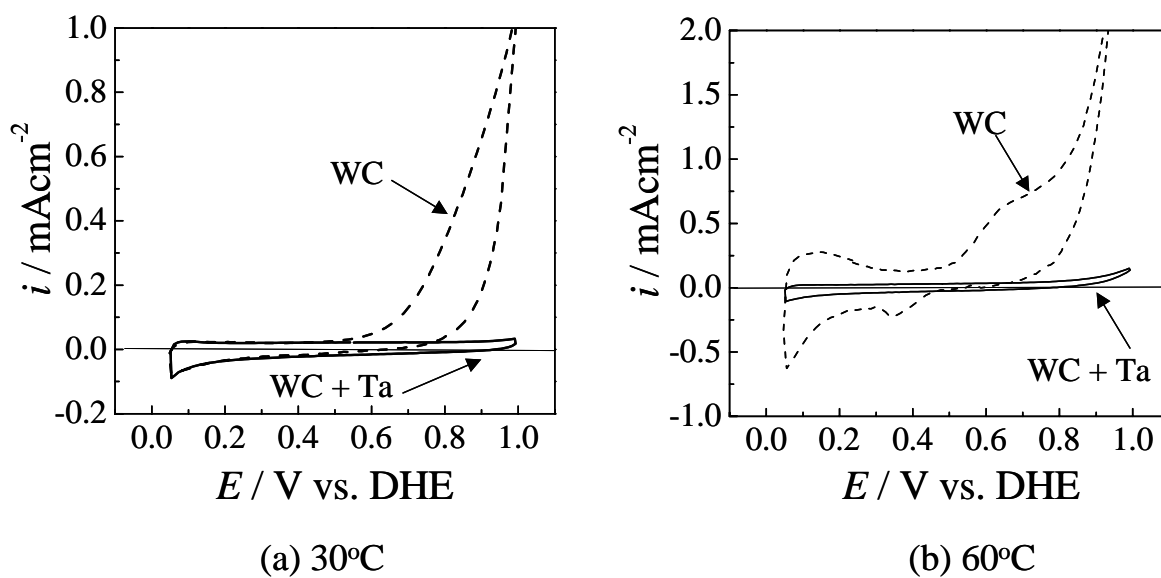


Fig. 4. Cyclic voltammograms under N_2 atmosphere ; scan rate=100mV/s.

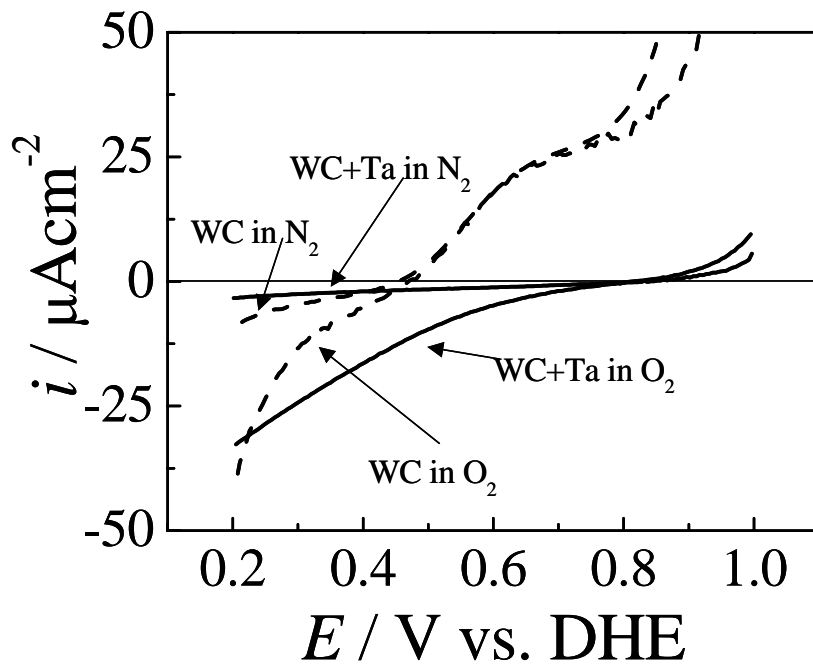


Fig. 5. Slow scan voltammograms for WC+Ta and WC ; scan rate= 5mV/s, 30°C.

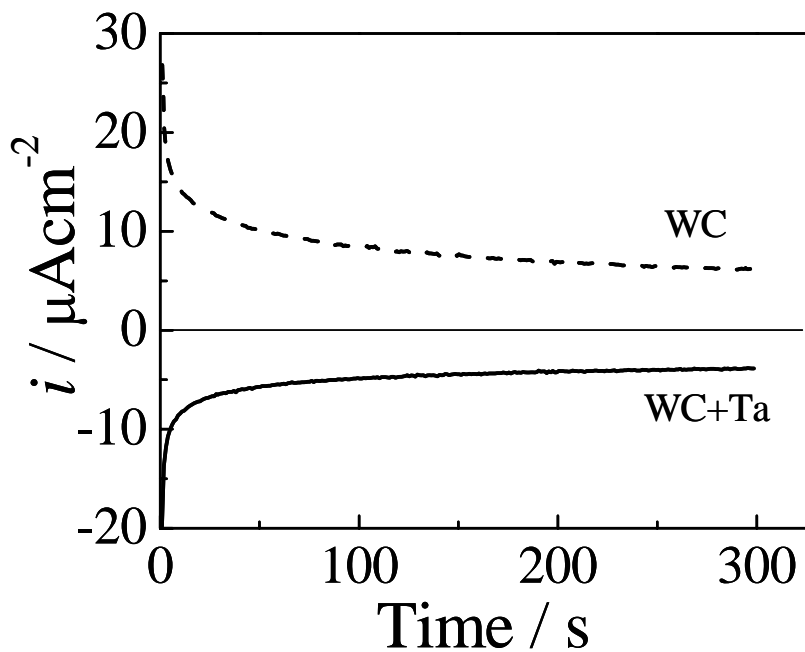


Fig. 6. Potentiostatic curves at 0.6V under O_2 atmosphere; 30°C.

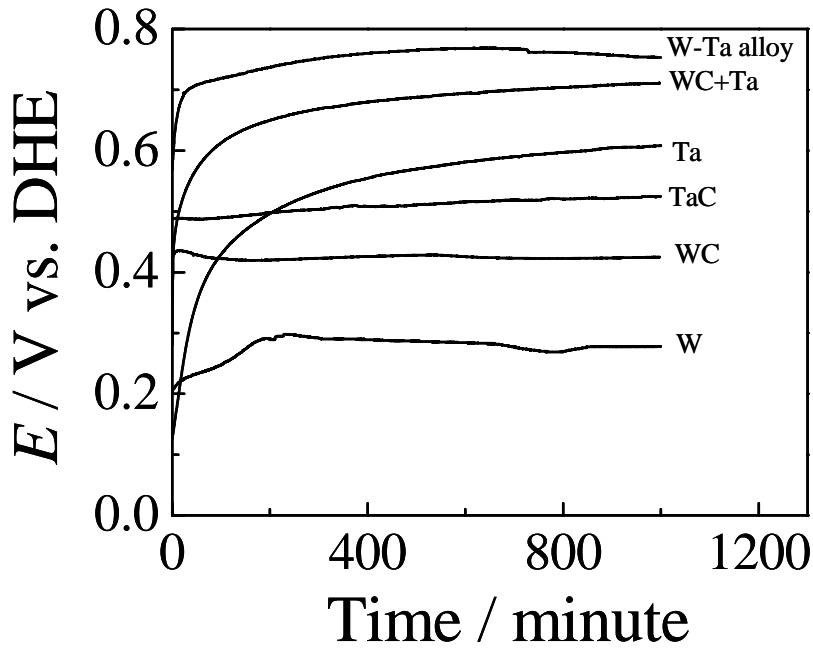


Fig. 7. Changes in open circuit potentials under O_2 atmosphere; $30^\circ C$.

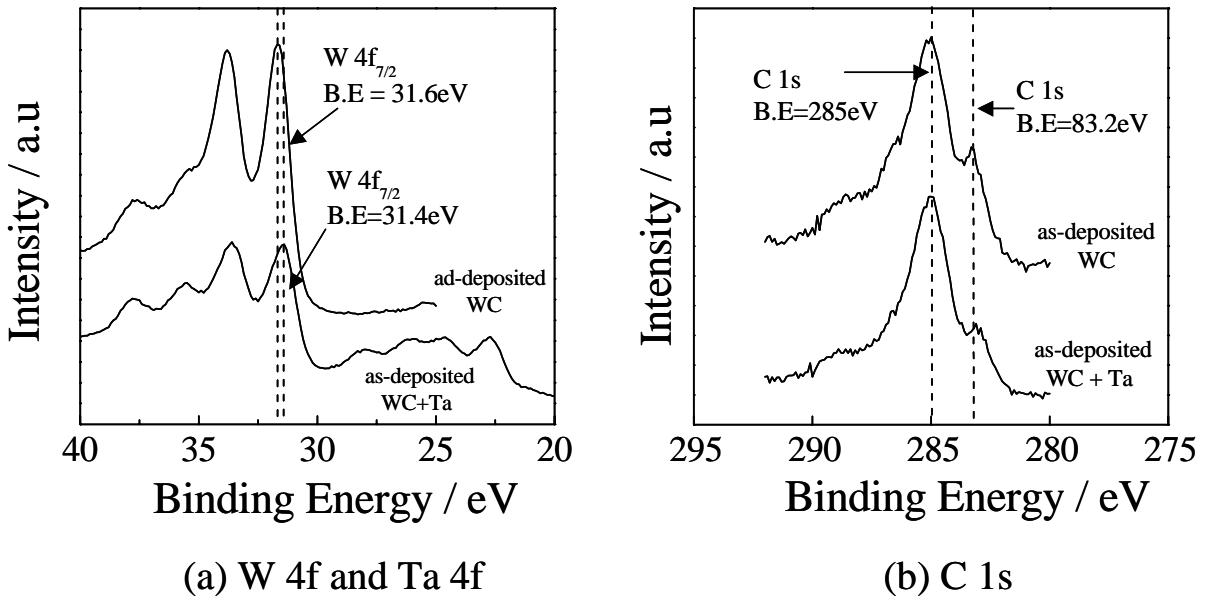


Fig. 8. XPS spectra for W 4f, Ta 4f and C 1s in WC and WC+Ta.

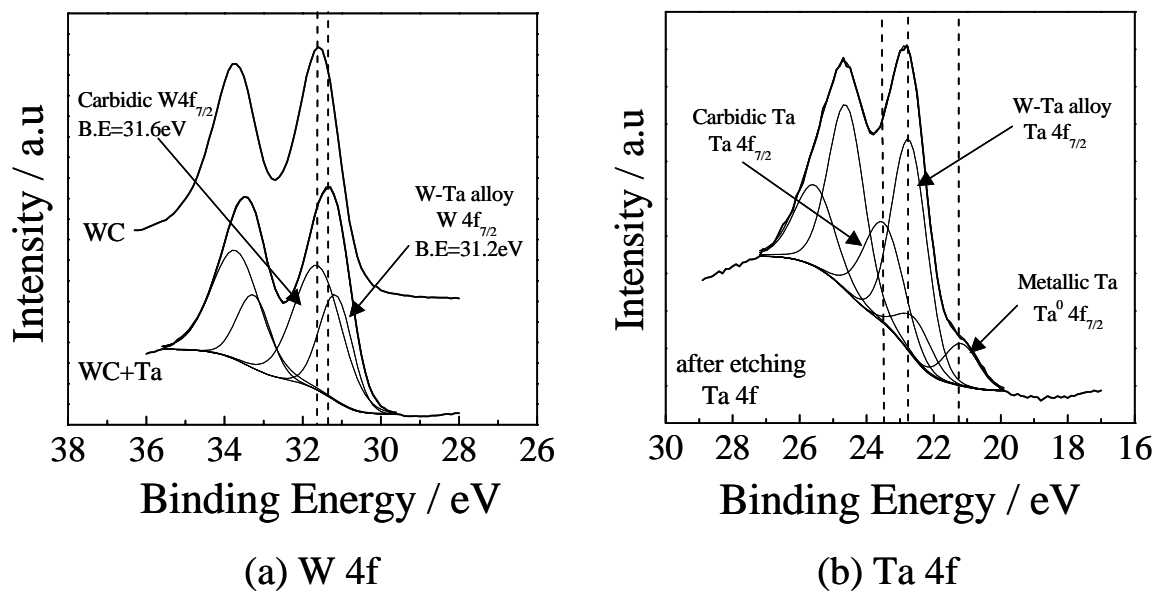


Fig. 9. XPS spectra for W 4f and Ta 4f after Ar⁺ etching.

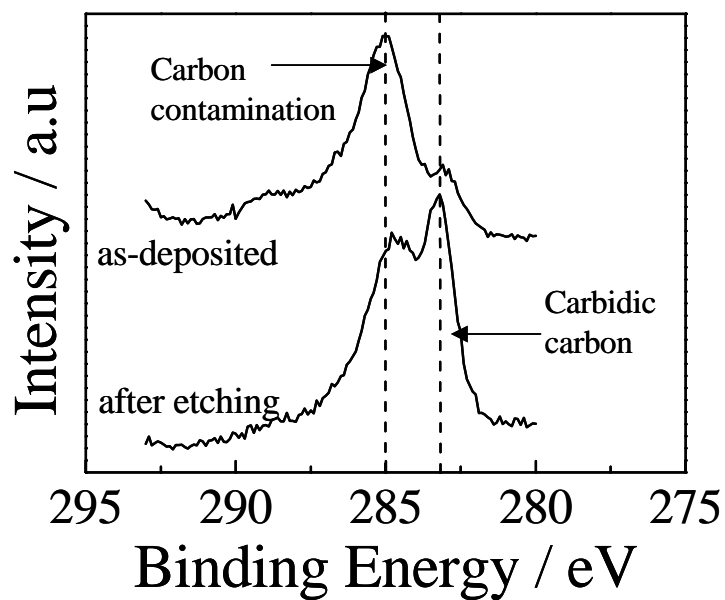


Fig.10. XPS spectra for C 1s peaks in WC+Ta after Ar⁺ etching.

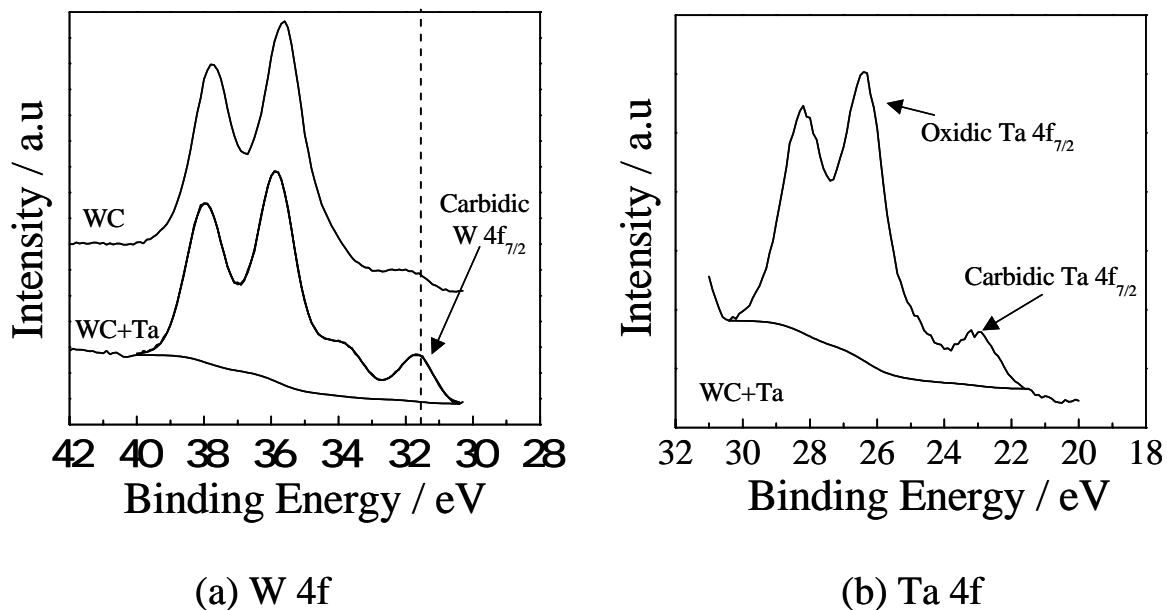


Fig. 11. XPS spectra for W 4f and Ta 4f after electrochemical measurements.

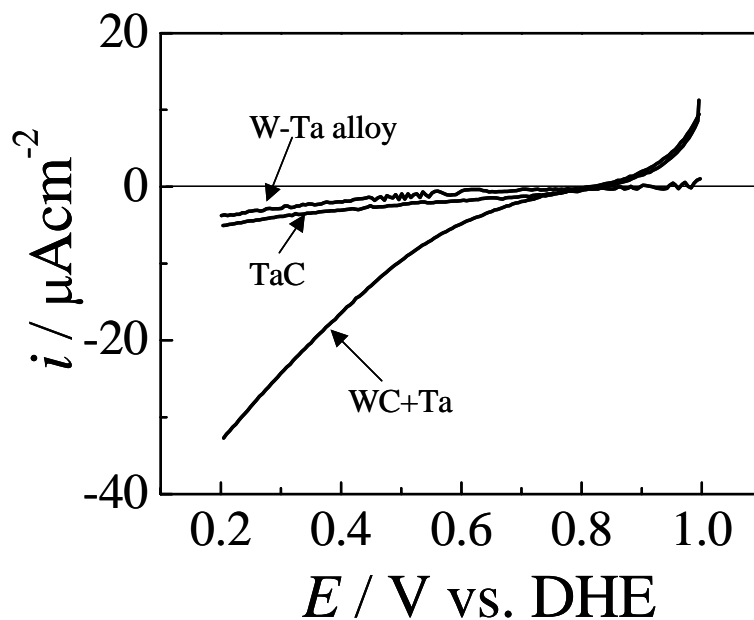


Fig. 12. Slow scan voltammograms under O_2 atmosphere; scan rate=5mV/s, 30°C.